J|A|C|S
ARTICLES
Published on Web 09/19/2006

A Point Mutation Converts Dihydroneopterin Aldolase to a Cofactor-Independent Oxygenase

Yi Wang,[‡] Gwynyth Scherperel,[§] Kade D. Roberts,[§] A. Daniel Jones,[‡,§] Gavin E. Reid,*[,§,‡] and Honggao Yan*[,‡]

Contribution from the Department of Biochemistry and Molecular Biology and Department of Chemistry, Michigan State University, East Lansing, Michigan 48824

Received May 17, 2006; E-mail: yanh@msu.edu; reid@chemistry.msu.edu

Abstract: Dihydroneopterin aldolase (DHNA) catalyzes the conversion of 7,8-dihydroneopterin (**1**) to 6-hydroxymethyl-7,8-dihydropterin (**4**) in the folate biosynthetic pathway. Substitution of a conserved tyrosine residue at the active site of DHNA by phenylalanine converts the enzyme to a cofactor-independent oxygenase, which generates mainly 7,8-dihydroxanthopterin (**6**) rather than **4**. **6** is generated via the same enol intermediate as in the wild-type enzyme-catalyzed reaction, but this species undergoes an oxygenation reaction to form **6**. The conserved tyrosine residue plays only a minor role in the formation of the enol reaction intermediate but a critical role in the protonation of the enol intermediate to form **4**.

Introduction

Dihydroneopterin aldolase (DHNA) catalyzes the conversion of 7,8-dihydroneopterin (**1**, Figure 1) to 6-hydroxymethyl-7,8-dihydropterin (**4**) in the folate biosynthetic pathway, one of principal targets for developing antimicrobial agents.[1] Like other enzymes, such as dihydropteroate synthase and dihydrofolate reductase, in the folate pathway,[2,3] DHNA is an attractive target for developing antimicrobial agents.[4] DHNA is also a unique aldolase in that it requires neither the formation of a Schiff base between the substrate and the enzyme nor metal ions for catalysis,[5] and in addition to the aldolase reaction, DHNA also catalyzes the epimerization at the 2′-carbon of **1** to generate 7,8-dihydromonapterin[6] (**5**). Interestingly, DHNAs from *Staphylococcus aureus* (SaDHNA) and *Escherichia coli* (EcDHNA), representatives of DHNAs from Gram-positive and Gram-negative bacteria, respectively, have significant differences in binding and catalytic properties.

One of the conserved residues at the active site of DHNA is a tyrosine residue, Y54 in SaDHNA and Y53 in EcDHNA. According to the crystal structure of SaDHNA in complex with **4**,[7] the pterin ring is stacked with the phenol ring of Y54 (Figure 2). The hydroxyl group of the phenol ring of Y54 is hydrogen-bonded to the amino group of the putative general base of K100 and the hydroxyl of the 6-hydroxymethyl group of the bound **4**. To investigate the role of the conserved tyrosine residue in catalysis, we replaced Y54 of SaDHNA and Y53 of EcDHNA with a phenylalanine residue by site-directed mutagenesis. The single-point mutations convert the aldolases to oxygenases, which generate mainly 7,8-dihydroxanthopterin (**6**) rather than

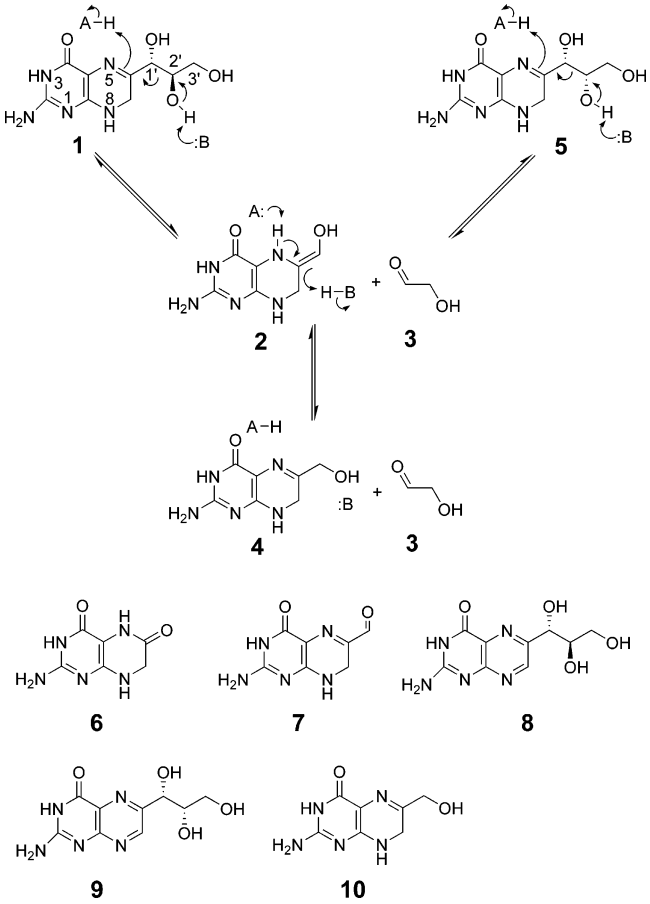

Figure 1. Reactions catalyzed by DHNA and related pterin compounds.

[‡] Department of Biochemistry and Molecular Biology.
[§] Department of Chemistry.

(1) Walsh, C. *Nat. Rev. Microbiol.* **2003**, *1*, 65−70.
(2) Bermingham, A.; Derrick, J. P. *Bioessays* **2002**, *24*, 637−648.
(3) Kompis, I. M.; Islam, K.; Then, R. L. *Chem. Rev.* **2005**, *105*, 593−620.
(4) Sanders, W. J.; et al. *J. Med. Chem.* **2004**, *47*, 1709−1718.
(5) Mathis, J. B.; Brown, G. M. *J. Biol. Chem.* **1970**, *245*, 3015−3025.
(6) Haussmann, C.; Rohdich, F.; Schmidt, E.; Bacher, A.; Richter, F. *J. Biol. Chem.* **1998**, *273*, 17418−17424.
(7) Hennig, M.; D'Arcy, A.; Hampele, I. C.; Page, M. G. P.; Oefner, C.; Dale, G. E. *Nat. Struct. Biol.* **1998**, *5*, 357−362.

10.1021/ja063455i CCC: $33.50

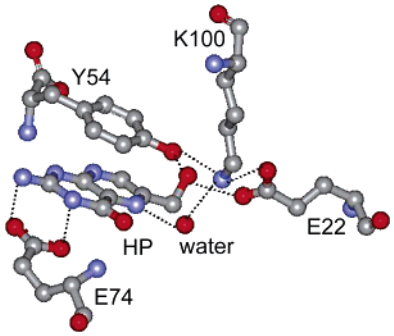

Figure 2. Polar interactions of **4** with SaDHNA.

4. **6** is generated via the same enol intermediate (**2**) as in the wild-type enzyme-catalyzed reaction, but this species undergoes an oxygenation reaction to form **6**. The conserved tyrosine residue plays only a minor role in the formation of the enol reaction intermediate but a critical role in the protonation of the enol intermediate to form **4**.

Experimental Procedures

Materials. Compounds **1**, **4**, **5**, **6**, **7** (6-formyl-7,8-dihydropterin), **8** (D-neopterin), **9** (L-monapterin), and **10** (6-hydroxymethylpterin) were purchased from Schircks Laboratories. Other chemicals were from Sigma or Aldrich. *Pfu* DNA polymerase was purchased from Strategene. Other molecular biology reagents were from New England Biolab.

Site-Directed Mutagenesis and Protein Purification. The mutants SaY54F and EcY53F, where Y54 of SaDHNA and Y53 of EcDHNA were replaced by a phenylalanine residue, respectively, were made by a polymerase chain reaction-based method using high-fidelity *pfu* DNA polymerase according to a protocol developed by Stratagene. The forward and reverse primers for making the SaY54F mutant were 5′-GTT ATTGATACAGTTCATTTTGGTGAAGTGTTCGAAGAG G-3′ and 5′-CCTCTTCGAACA CTTCACCAAAATGAACTGTATCAA-TAAC-3, respectively. The forward and reverse primers for making the EcY53F mutant were 5′-CGGATTGCCTCAGTTTCGCTGACAT-TGCAGAAAC-3′ and 5′-GTTTCTGCAATGTCAGCGAAACTGAG-GCAATCCG-3′, respectively. The mutants were selected by DNA sequencing. To ensure that there were no unintended mutations in the mutants, the entire coding sequences of the mutated genes were determined.

The mutant proteins were purified as previously described (Wang et al., unpublished). Briefly, SaY5F was purified to homogeneity by a Ni-NTA column followed by a Bio-Gel A-0.5m gel column (Bio-Rad). EcY53F was purified by a (diethylamino)ethyl−cellulose column (Whatman) followed by a Bio-Gel A-0.5m gel column. The purities of the protein preparations were checked by sodium dodecyl sulfate−polyacrylamide gel electrophoresis. The amino acid sequences of the purified proteins were confirmed by "top-down" tandem mass spectrometry.[8] The purified proteins were concentrated, dialyzed, lyophilized, and stored at −80 °C.

Equilibrium Binding Studies. The procedures for the equilibrium binding studies of DHNAs were essentially the same as previously described for the similar studies of 6-hydroxymethyl-7,8-dihydropterin pyrophosphokinase using a Spex FluoroMax-2 fluorometer.[9,10] Briefly, proteins and ligands were all dissolved in 100 mM Tris-HCl, pH 8.3, and the titration experiments were performed in a single cuvette with a Spex FluoroMax-2 fluorometer at 24 °C. To determine the K_d values of the binding of **8** and **9** to SaY54F, a 2 mL solution containing 10 μM SaY54F was titrated with a stock solution of **8** or **9**. To determine the K_d values of the binding of **10** to SaY54F and the binding of **8**, **9**, and **10** to EcY53F, a 2 mL solution containing 1 μM of one of the ligands (**8**, **9**, or **10**) was titrated with a stock solution of SaY54F or EcY53F. The K_d values were obtained by nonlinear least-squares fitting of the titration data as previously described.[9]

Stopped-Flow Analysis. Stopped-flow experiments were performed on an Applied Photophysics SX.18MV-R stopped-flow spectrofluorometer at 25 °C. One syringe contained the protein (SaY54F or EcY53F), and the other contained **8**, **9**, or **10**. The protein concentration was 1 or 2 μM, and the ligand concentrations ranged from 5 to 60 μM. All concentrations reported are those after the mixing of the two syringe solutions. Fluorescence traces were obtained with an excitation wavelength of 360 nm and a filter with a cutoff of 395 nm for emission. Apparent rate constants were obtained by nonlinear least-squares fitting of the data to a single-exponential equation and were replotted against the ligand concentrations. The association and dissociation constants were obtained by linear regression of the apparent rate constants vs ligand concentration data.

Kinetic Assay. The kinetic experiments were performed manually. Both **1** and DHNA were dissolved in a buffer containing 100 mM Tris-HCl, 1 mM ethylenediaminetetraacetic acid, and 5 mM dithiothreitol, pH 8.3. The reactions were initiated by the addition of DHNA and stopped with 1 N HCl. The stopped reaction mixtures were processed and separated by HPLC as previously described.[6]

NMR Spectroscopy. NMR measurements were made at 25 °C with a Varian Inova 600 spectrometer. The initial NMR sample contained 1 mM **1** and 1 mM tris(2-carboxyethyl) phosphine (TCEP) in 100 mM sodium phosphate buffer, pH 8.3 (pH meter reading without correction for deuterium isotope effects), made with 90% H_2O and 10% D_2O. The reaction was initiated with 1 μM SaDHNA or 3 μM SaY54F. NMR spectra were recorded before and after the addition of the enzyme. The spectral width for the NMR data was 12000 Hz, with the carrier frequency at the HDO resonance. The solvent resonance was suppressed by presaturation. Each FID was composed of 16K data points with 64 transients. The delay between successive transients was 1.7 s. The time domain data were processed by zero-filling to 32K points, exponential multiplication (1 Hz), and Fourier transformation. Chemical shifts were referenced to the internal standard sodium 2-dimethyl-2-silapentane-5-sulfonate sodium salt.

Mass Spectrometry (MS). All MS experiments were performed using a Thermo model LTQ linear ion trap mass spectrometer. The initial 300 μL samples contained 200 μM **1** and 4 μM SaDHNA or 10 μM SaY54F in 5 mM ammonium carbonate, pH 8. Twenty-microliter aliquots of the reaction mixtures were taken out at 1-min intervals and mixed with 80 μL of a solution containing 1% acetic acid and 50% methanol. The samples were further diluted with the same solution and then introduced into the mass spectrometer at a flow rate of 0.5 μL/min by nanoelectrospray ionization (nESI). The following nESI conditions were used: spray voltage, 1.8 kV; heated capillary temperature, 200 °C; capillary voltage, −10 V; and tube lens voltage, −50 V. Collision-induced dissociation (CID) tandem mass spectrometry (MS/MS and MS^3) spectra were acquired at an activation q value of 0.25 using an isolation width of 1 or 2 Da (to monoisotopically isolate the precursor ion), a normalized collision energy of 30−40%, and an activation time of 30 or 300 ms. The values were chosen such that the gentlest conditions were used in order to completely dissociate the selected precursor ion (i.e., some precursor ions required a larger normalized collision energy and/or longer activation time). The MS, MS/MS, and MS^3 product ion spectra shown are the averages of 60 individual mass analysis scans.

Gas Chromatography/Mass Spectrometry (GC/MS) of Glycolaldehyde (3). The derivatization protocol is a modified version of a procedure developed for analysis of plant metabolites,[11] with *N*-(*tert*-butyldimethylsilyl)-*N*-methyltrifluoroacetamide (MTBSTFA) substituted for *N*-methyl-*N*-(trimethylsilyl)trifluoroacetamide as needed to form *tert*-

(8) Scherperel, G.; Yan, H. G.; Wang, Y.; Reid, G. E. *Analyst* **2006**, *131*, 291−302.
(9) Li, Y.; Gong, Y.; Shi, G.; Blaszczyk, J.; Ji, X.; Yan, H. *Biochemistry* **2002**, *41*, 8777−8783.
(10) Shi, G.; Gong, Y.; Savchenko, A.; Zeikus, J. G.; Xiao, B.; Ji, X.; Yan, H. *Biochim. Biophys. Acta* **2000**, *1478*, 289−299.

butyldimethylsilyl (TBDMS) ether derivatives instead of the trimethylsilyl derivatives that were reported previously. The advantage is that the TBDMS derivatives give more conclusive evidence of the product's molecular mass in the form of a strong $[M - 57]^+$ ion in the mass spectrum. The reaction contained 200 μM **1** and 4 μM SaDHNA or 6.3 μM SaY54F in 5 mM ammonium carbonate, pH 8.3. The reaction was stopped after 20 min by adding 1 N HCl and centrifuged for 5 min with a microcentrifuge. The supernatant collected was then lyophilized overnight to dryness. The dried residue was incubated for 1 h with 10 μL of methoxyamine hydrochloride in pyridine (10 mg/mL) and MTBSTFA. GC/MS analyses were performed on an Agilent 5973 mass spectrometer coupled to a model 6890 gas chromatograph. All analyses were performed using 70 eV electron ionization. Separations were performed using a 30 m HP-5MS column and helium (36 cm/s) as carrier gas. The column temperature was programmed from 50 (4 min hold) to 285 °C at 10 deg/min.

HPLC Identification of Formic Acid. Formic acid was identified as previously described.[12] One-milliliter reaction mixtures contained 200 μM **1** and 10 μM SaDHNA or SaY54F in 100 mM HEPES−KOH, pH 8.3, and were mixed with 100 μL of 3.2 M H_2SO_4 after 20 min of incubation at 24 °C. The solutions were centrifuged, filtered through a 0.45 μm syringe filter, and injected into a 7.8 mm × 300 mm Aminex HPX-87H column. Standard compounds, including formic acid, acetic acid, glycolic acid, glyceric acid, succinic acid, formaldehyde, glycolaldehyde (**3**), and glyceraldehyde, were treated the same way as the enzymatic reaction mixture. The column was eluted with 4 mM H_2SO_4 at a flow rate of 0.6 mL/min, and the elution was monitored by a Waters 2487 UV detector at 210 nm and a Waters 410 differential refractometer.

Oxygen Consumption Assay. Oxygen consumption was measured using a Gilson 5/6H oxygraph with a Clark oxygen electrode at 25 °C as previously described.[13] The initial 1.8 mL samples contained 200 μM **1** in 100 mM HEPES−KOH, pH 8.2. The reactions were initiated by 8 μM SaDHNA or SaY54F at 25 °C. The turnover number for SaY54F was calculated using the slope of the initial linear part of the data obtained by linear regression.

Results

Biochemical Analysis. Previously we established the thermodynamic and kinetic framework for the structure−function studies of SaDHNA and EcDHNA (Wang et al., unpublished). We performed the biochemical characterizations of the mutants SaY54F and EcY53F using the same strategy. The binding steps were mimicked with the substrate and product analogues **8**, **9**, and **10**. The only difference between the substrate and product analogues and the corresponding substrate and products is that between C7 and N8 is a double bond in the analogues and a single bond in the substrate and products. **8**, **9**, and **10** are excellent substrate and product analogues (Wang et al., unpublished). The K_d values were measured by equilibrium binding experiments using fluorometry. The association and dissociation rate constants were determined by kinetic binding experiments using stopped-flow fluorometry. Representative results are shown in Figures S1 and S2 for the equilibrium and kinetic binding experiments, respectively. The complete results are summarized in Table 1. For SaY54F, the mutation increased the affinities of the ligands for the enzyme by a factor of ∼4−6. For EcY53F, the mutation increased the affinities of **8** and **9** by a factor of 4−6, but decreased the affinity of **10** by a factor of 4. The changes were mainly caused by the changes in the dissociation rate constants. The results suggested that neither the hydroxyl of Y54 of SaDHNA nor that of Y53 of EcDHNA is critically important for the binding of substrate or products. To our surprise, there was a dramatic drop in the total fluorescence intensity in the HPLC analysis of the reaction mixtures generated by either SaY54F or EcY53F as the reaction progressed, suggesting that the substrate was converted to a nonfluorescent compound at the chosen excitation and emission wavelengths and the mutant enzyme-catalyzed reactions generated different products.

Table 1. Binding Constants of *S. aureus* and *E. coli* DHNAs and Y→F Mutants[a]

		SaDHNA	SaY54F	EcDHNA	EcY53F
8	K_d	18 ± 2	4.5 ± 0.9	0.77 ± 0.06	0.20 ± 0.01
	k_1	0.24 ± 0.01	0.099 ± 0.005	0.32 ± 0.02	0.26 ± 0.01
	k_{-1}	4.5 ± 0.1	0.44 ± 0.05	0.29 ± 0.03	0.060 ± 0.006
9	K_d	13 ± 1	3.7 ± 0.5	2.6 ± 0.06	0.40 ± 0.01
	k_1	0.29 ± 0.02	0.13 ± 0.01	0.26 ± 0.01	0.28 ± 0.01
	k_{-1}	4.2 ± 0.2	0.80 ± 0.09	0.58 ± 0.03	0.11 ± 0.01
10	K_d	24 ± 0.2	3.8 ± 0.9	0.10 ± 0.01	0.40 ± 0.02
	k_1	0.45 ± 0.02	0.68 ± 0.01	0.55 ± 0.04	0.79 ± 0.01
	k_{-1}	10 ± 0.5	2.9 ± 0.06	0.062 ± 0.001	0.26 ± 0.01

[a] K_d in μM, k_1 in μM^{-1} s^{-1}, and k_{-1} in s^{-1}.

NMR Analysis. To identify the products of the mutant-catalyzed reactions, we analyzed the reaction mixtures by NMR. Representative spectra are shown in Figure 3, and the chemical shifts of selected protons of related compounds are summarized in Table 2. As shown in Figure 3, **3** was generated by both the wild-type enzyme- and the mutant-catalyzed reactions. While the wild-type enzyme-catalyzed reaction generated **4** along with **3** (Figure 3A), the mutant-catalyzed reaction generated little **4** (Figure 3B). The major product of the mutant-catalyzed reaction was a compound with a proton peak at 4.12 ppm, which was identified as **6**, as detailed in the following section; **6** was a minor product in the wild-type enzyme-catalyzed reaction. The NMR spectra of the reaction mixtures generated by the *E. coli* enzymes (data not shown) were very similar to those of the reaction mixtures generated by the *S. aureus* enzymes. Because both SaDHNA and SaY54F were saturated with the substrate **1** under the experimental conditions, their turnover numbers (k_{cat}) could be calculated on the basis of the enzyme concentration, the initial substrate concentration, and the NMR peak intensities of the substrate and products. The calculated k_{cat} values for the formation of **4** and **6** were 0.20 and 5.7×10^{-3} s^{-1}, respectively, for SaDHNA, and 3.4×10^{-4} and 0.018 s^{-1}, respectively, for SaY54F. The rate for the formation of **6** was ∼3% of that for the formation of **4** in the SaDHNA-catalyzed reaction. The relative rates were reversed in the SaY54F-catalyzed reaction, and the rate for the formation of **4** was ∼2% of that for the formation of **6**.

MS Analysis. The identity of the major product of the SaY54F-catalyzed reaction that gave rise to the 4.12 ppm peak in the NMR spectrum could not be determined by 1D proton NMR spectroscopy. To identify the reaction product, we analyzed the reaction mixtures generated by both the wild-type and the mutant enzymes by MS. As expected, the primary product generated by SaDHNA was different from that generated by SaY54F (Figure 4). The mass spectrum of the reaction involving SaDHNA showed the formation of a product ion at

(11) Roessner, U.; Wagner, C.; Kopka, J.; Trethewey, R. N.; Willmitzer, L. *Plant J.* **2000**, *23*, 131−142.
(12) McKinlay, J. B.; Zeikus, J. G.; Vieille, C. *Appl. Environ. Microbiol.* **2005**, *71*, 6651−6656.
(13) Bratton, M. R.; Pressler, M. A.; Hosler, J. P. *Biochemistry* **1999**, *38*, 16236−16245.

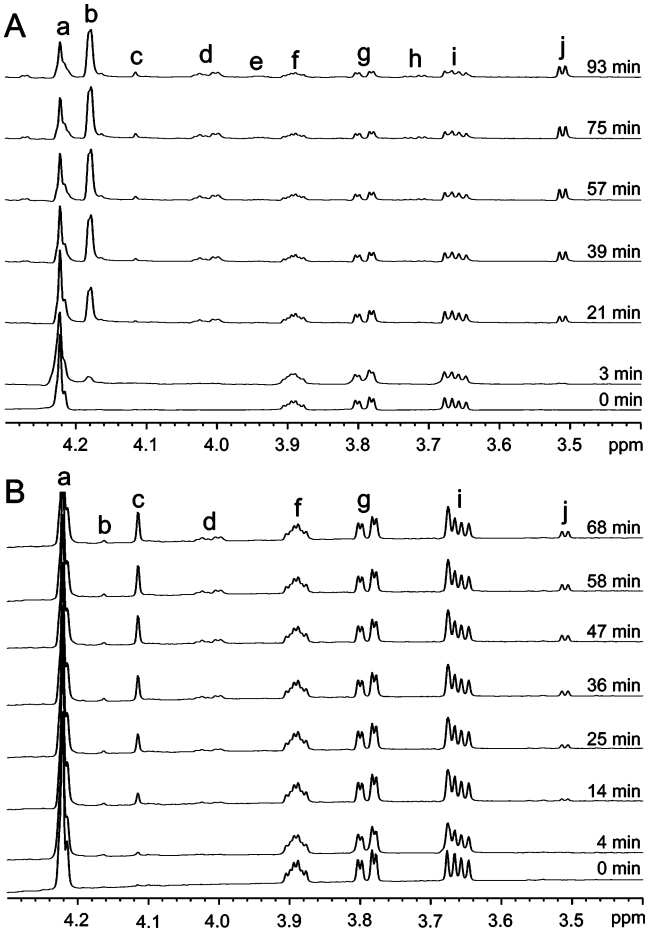

Figure 3. NMR analysis of the reactions catalyzed by SaDHNA (A) and SaY54F (B). The initial NMR sample contained 1 mM **1** and 1 mM TCEP in 100 mM sodium phosphate buffer, pH 8.3, made with 90% H_2O and 10% D_2O. The reaction was initiated with 1 μM SaDHNA (A) or 3 μM SaY54F (B). Peak identities are as follows: a, 7H and 1′H of **1**; b, 7H and the 6-hydroxymethyl group of **4**; c, 7H of **6**; d, from **3** and TCEP; e, 2′H of **5**; f, 2′H of **1**; g, 3′Ha of **1**; h, 3′Ha of **5**; i, 3′Hb of **1** and **5**; and j, from **3**.

Table 2. Chemical Shifts of Selected Protons of Compounds Related to the Reactions Catalyzed by the Wild-Type and Mutant DHNAs[a]

compds	7H	1′H	2′H	3′Ha	3′Hb	other
1	4.22 (d)	4.22 (d)	3.90 (m)	3.80 (m)	3.66 (m)	
5	4.22 (d)	4.27 (d)	3.94 (m)	3.72 (m)	3.66 (m)	
4	4.18 (s)					4.18 (s)
6	4.12 (s)					
3						3.50 (d)
3 + TCEP						4.02 (m)

[a] The chemical shifts were from those of the commercial compounds in 50 mM sodium phosphate buffer, pH 8.3 (pH meter reading without correction for deuterium isotope effects), made with 90% H_2O and 10% D_2O. The peak at 4.02 ppm was present only in the presence of both **3** and TCEP. The 4.18 ppm peak of **4** also belongs to the 6-hydroxymethyl group.

m/*z* 196, while the spectrum of the reaction involving SaY54F showed the formation of a product ion at *m*/*z* 182.

To determine the identity of the *m*/*z* 196 ion in Figure 4A, MS/MS and MS^3 spectra were obtained and compared to those of the expected reaction product **4**. As shown in Figure S3, the major ions observed by CID MS/MS of the ion at *m*/*z* 196 obtained from the SaDHNA-catalyzed reaction were identical to the major product ions seen in the MS/MS product ion

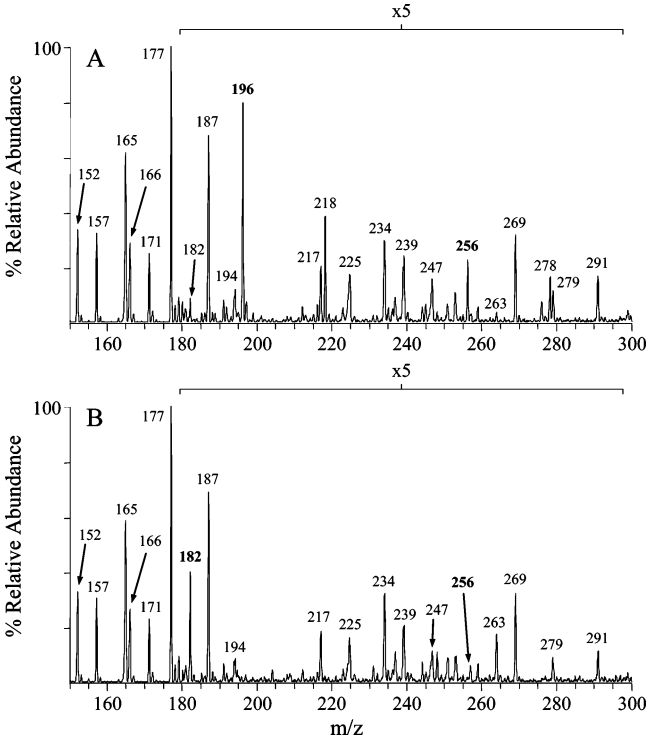

Figure 4. ESI-MS analysis of the mixtures generated by a 10 min reaction of SaDHNA (A) and SaY54F (B). The substrate **1** is observed at *m*/*z* 256 in both spectra. The region from *m*/*z* 180−300 has been magnified (×5) for clarity.

spectrum obtained from the standard (compare parts A and B of Figure S3). The most abundant product ion in both parts A and B of Figure S3 at *m*/*z* 178 is most likely due to the loss of water from the precursor ion. To obtain further confirmation of the expected product ion structure, MS^3 was then performed on the *m*/*z* 178 product ion (Figure S3C,D). As expected, the experimental and standard MS^3 spectra were essentially identical. The most abundant product ions at *m*/*z* 161 and 150 are most likely due to the loss of NH_3 and CO, respectively. Based on an MS^4 experiment (data not shown), the MS^3 product ion seen at *m*/*z* 179 was formed via an ion−molecule reaction between the ion at *m*/*z* 161 and a water molecule. Taken together, the MS/MS and MS^3 spectra provided strong evidence that the product seen at *m*/*z* 196 from the reaction of **1** with SaDHNA is **4**.

This same type of analysis was also performed in order to determine the identity of the *m*/*z* 182 ion in Figure 4B. MS/MS and MS^3 spectra of the ion were obtained and compared to those of the proposed reaction product, **6**. An examination of Figure S4 indicated that the major ion observed by CID MS/MS of the ion at *m*/*z* 182 obtained from the SaY54F-catalyzed reaction is identical to the major ion seen in the MS/MS product ion spectrum obtained from the standard (compare parts A and B of Figure S4). The *m*/*z* 154 product ion in both parts A and B of Figure S4 is most likely due to the loss of CO from the precursor ion. MS^3 was then performed on the *m*/*z* 154 ion (Figure S4C,D). Again, the experimental and standard spectra were essentially the same. The major MS^3 product ion, seen at *m*/*z* 126, corresponds to the loss of CO, while the second most intense ion, seen at *m*/*z* 137, corresponds to the loss of NH_3. As was the case for the previous analysis of the SaDHNA-catalyzed reaction, these spectra together provided strong

evidence that the product seen at *m*/*z* 182 from the reaction of **1** with SaY54F is **6**.

The *m*/*z* 256 ion (Figure 4) was found to correspond to **1** (Figure S5), as well as probably partly due to **5**, which was generated by the enzymatic reactions. **1** and **5** differ only in the stereochemistry of their 2′-carbons and have the same molecular weight. The *m*/*z* 194 ion (Figure 4) was found to correspond to **10** and **7**, because the MS/MS and MS^3 spectra of the *m*/*z* 194 species were the sums of those of **10** and **7** standards, with **10** contributing more than **7** (Figure S6). The existence of **7** was also confirmed by spectrophotometry, in which **7** has a characteristic absorption peak at 420 nm (data not shown).

GC/MS Confirmation of 3. Since the major product of the SaY54F-catalyzed reaction was **6**, not **4**, it was necessary to confirm the identity of **3** as indicated by the NMR analysis (Figure 3). To this end, we derivatized the reaction products of SaDHNA and SaY54F with methoxyamine and MTBSTFA to form the *tert*-butyldimethylsilyl ether of the methoxime. **3** was then detected by GC/MS as shown in Figure S7. The enzymatic reaction product (Figure S7B) was identified by comparison with the commercially available standard compound (Figure S7A). The retention time of the standard is 12.3 min (data not shown). The molecular weight of its derivative is 203 Da, but the molecular ion was too weak to be observed, as is typical for these derivatives. The dominant fragment ions in the mass spectrum appeared at *m*/*z* 146 ($[M - C_4H_9]^+$) and 188 ($[M - CH_3]^+$). The two reaction mixtures generated by SaDHNA and SaY54F both contained a peak with the same retention time as that of the standard **3**. The mass spectrum of the derivative (the peak at 12.3 min) from the SaY54F-catalyzed reaction (Figure S7B), which was identical to that of the SaDHNA-catalyzed reaction (data not shown), also showed two dominant ions at *m*/*z* 146 and 188. This result and that of the NMR analysis clearly indicated that the SaY54F-catalyzed reaction generates **3**, as does the SaDHNA-catalyzed reaction.

HPLC Identification of Formic Acid. Because **6** contains one carbon less than **4**, the SaY54F-catalyzed reaction must generate a one-carbon species, most likely formic acid. To identify the one-carbon species, we analyzed the 7,8-dihydro-D-neopterin (DHNP) reaction mixtures generated by SaDHNA and SaY54F by HPLC using an Aminex HPX-87H column. The unknown compounds in the reaction mixtures were identified by comparing their retention times with those of the standard compounds, as shown in Figure S8. This HPLC run of standard compounds (blue line) included succinic acid at 13.5 min, formic acid at 14.9 min, and acetic acid at 16 min. It also showed a peak at 17.5 min, probably due to the HEPES buffer, which also appeared in all chromatograms, including those of the SaY54F solution (green line), the reaction mixture generated by SaY54F (red line), the reaction mixture generated by SaDHNA (cyan line), and the buffer alone (data not shown). The chromatogram of the reaction mixture generated by SaY54F showed an intense peak at 14.9 min, which was the same as the retention time for standard formic acid. The small shoulder at the left side was probably due to the protein. The intense peak in the chromatogram of the reaction mixture generated by SaY54F was absent in the chromatogram of the reaction mixture generated by SaDHNA. The result indicated that the mutant-catalyzed reaction generates formic acid but the wild-type enzyme-catalyzed reaction does not.

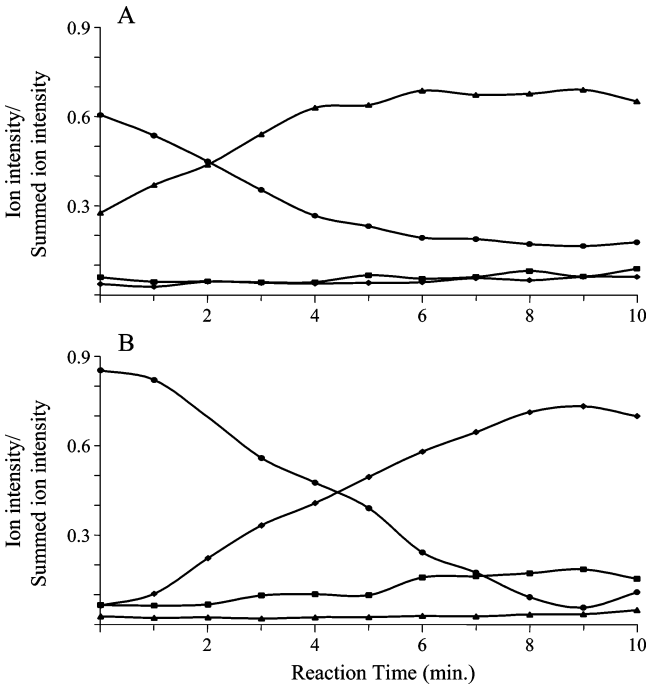

Figure 5. ESI-MS time course analysis of the DHNP reactions catalyzed by SaDHNA (A) and SaY54F (B). (●, *m*/*z* 256; ■, *m*/*z* 194; ▲, *m*/*z* 196; ◆, *m*/*z* 182).

Is 6 Derived from 4? Since the C1′−C2′ bond is cleaved first in the generation of DXHP, which is the same for the normal aldolase reaction for the formation of **4**, it is logical to ask whether **6** is derived from **4**. To address this question, we analyzed the time course of the DHNP reaction by MS. The results are shown in Figure 5. The ions at *m*/*z* 256, 196, and 182 were due to **1**, **4**, and **6**, respectively, as described earlier. The *m*/*z* 194 ions were due to a large part from **10** and to a small part from **7**. The results showed again that the major product of the wild-type enzyme-catalyzed reaction was **4** as expected, but the major product of the mutant-catalyzed reaction was **6**. Furthermore, there was no accumulation of **4** in the mutant-catalyzed reaction, suggesting that **6** was not derived from **4**, unless the conversion of **4** to **6** was much faster than the formation of **4**. To confirm that **6** was not formed from the rapid conversion of **4**, **4** was incubated with SaY54F and analyzed by MS. If **6** was derived from the rapid conversion of **4**, then over time these spectra should show a decrease in the intensity of *m*/*z* 196 and an increase in the intensity of *m*/*z* 182. There was not, however, any production of the ion at *m*/*z* 182 seen in these spectra (not shown), indicating that DXHP was not derived from **4**.

The Source of Oxygen. Finally, we considered the source of the new oxygen at the C6 position of **6**. Was it from water or from molecular oxygen dissolved in the buffer? To address this issue, we ran the DHNP reaction in buffer prepared with ^{18}O-water and analyzed the reaction mixture with MS. With ^{18}O-water, if the oxygen was from the solvent, the mass spectrum should show a shift in the *m*/*z* of the protonated product ion from 182 to 184. The MS spectra of the reaction mixtures obtained with ^{18}O-water as the solvent, however, were the same as the spectra obtained when the reaction was run in unlabeled solvent (data not shown), indicating that there was

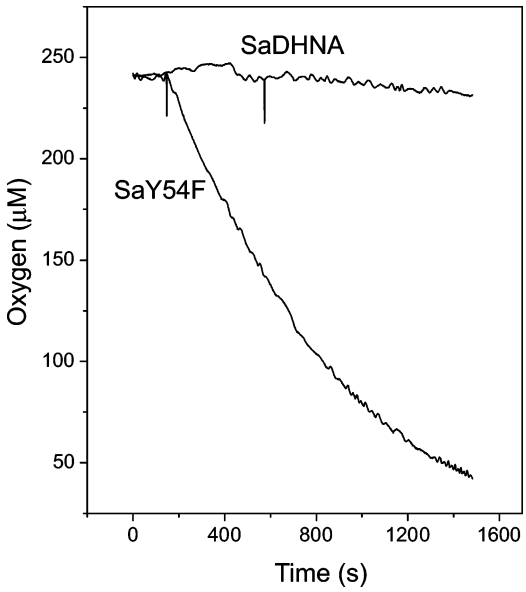

Figure 6. Oxygen consumption by the reactions catalyzed by SaDHNA and SaY54F. The initial samples contained 200 μM **1** in 100 mM HEPES−KOH, pH 8.2, and the reactions were initiated by 8 μM SaDHNA or SaY54F as marked by the vertical lines.

no ^{18}O incorporation in any of the products and the oxygen incorporated in the product **6** does not come from water. We then measured the oxygen consumption of the reactions catalyzed by SaY54F and SaDHNA. The results are shown in Figure 6. The amounts of wild-type and mutant enzymes were both 8 μM. Under the conditions, nearly all of substrate **1** was converted to products. The results showed that only the mutant-catalyzed reaction consumes a significant amount of oxygen, indicating that SaY54F is an oxygenase and the source of oxygen for the oxygenation reaction is molecular oxygen dissolved in the buffer. We calculated the turnover number for the oxygenation reaction from the linear portion of the oxygen consumption curve, which was 0.027 s^{-1}, in close agreement with the turnover number for the formation of **6** calculated from the NMR time course of the SaY54F-catalyzed reaction (0.018 s^{-1}), indicating that one oxygen molecule is used in the formation of one molecule of **6**. The extra oxygen consumption was probably due to the formation of **7** and **10**.

Discussion

SaY54F and EcY53F Are Oxygenases. By a variety of means, we have shown that the major product of the mutant (either SaY54F or EcY53F)-catalyzed reaction is **6**, rather than **4** as in the wild-type enzyme-catalyzed reaction. The turnover number for the formation of **6** is >50-fold that for the formation of the normal product **4** for SaY54F. The initial clue to the surprising properties of the mutant enzymes was a dramatic drop of the fluorescence intensities of the reaction mixtures. The NMR analysis of the reaction mixtures revealed that the mutant enzymes generate a new compound with a ^1H NMR signal at 4.12 ppm and little of the normal product **4** (Figure 3). The new compound was also a major product in the MS analysis of the reaction mixtures generated by the mutant SaY54F (Figure 4) and was identified to be **6** by comparing its MS/MS and MS^3 spectra with those of its standard (Figure S4). This raises the immediate question of how **6** is generated. Is **6** generated via the cleavage of the C6−C1′ bond or the C1′−C2′ bond as in the aldolase reaction? The fact that either mutant-catalyzed reaction generates GA, and furthermore that about equal moles of GA and **6** are generated (Figure 5), strongly indicates that **6** is generated via the cleavage of the C1′−C2′ bond. The formation of GA was confirmed by the derivatization of the reaction mixtures followed by GC/MS analysis (Figure S7). Since the first step in the generation of **6** is the cleavage of the C1′−C2′ bond, as in the wild-type enzyme-catalyzed reaction, the next question is whether **6** is derived from **4**. The MS analysis of the time course of the mutant-catalyzed reaction shows that there is no accumulation of **4** in the reaction (Figure 5). This indicates that **6** is not derived from **4**, unless the conversion of **4** to **6** is very rapid relative to the generation of **4**. This was addressed by mixing standard **4** with the mutant and following the possible reaction by MS. The result indicates that **4** cannot be converted to **6** under the experimental conditions. Since the cleavage of the C1′−C2′ bond generates an intermediate with one carbon more than **6**, the conversion of the intermediate to **6** must generate a one-carbon species, which was identified as formic acid by comparing the HPLC chromatograms of the reaction mixtures generated by the mutant and wild-type enzymes with those of standard organic acids and aldehydes (Figure S8). The remaining question is where the oxygen atom at the C6 position of **6** comes from. Is it from water or from oxygen molecules dissolved in the buffer? This issue was addressed by the ^{18}O-water experiment and the oxygen consumption assay. The ^{18}O-water experiment eliminates water as the source for the oxygen newly attached to the pterin ring. The oxygen consumption assay indicates that molecular oxygen is the source for the oxygenation reaction, because significant oxygen consumption occurs only in the mutant-catalyzed reaction (Figure 6) and the turnover number calculated from the oxygen consumption data is comparable to that for the formation of **6** calculated from the NMR data.

The above analysis leads us to propose a chemical mechanism for the mutant-catalyzed reaction, as depicted in Figure 7. The initial step in the formation of **6** is the generation of the same enol intermediate as in the wild-type enzyme-catalyzed reaction, which involves the cleavage of the C1′−C2′ bond and yields approximately equal moles of GA and **6**, as described earlier. Deprotonation of N5 of the enol intermediate generates a carbanion species, which donates a single electron to molecular oxygen to form a caged radical pair. The caged radicals react to generate the peroxide ion, which leads to the formation of **6** and formic acid. The participation of molecular oxygen in the mutant-catalyzed reaction has been confirmed by the oxygen consumption assay. The reaction path for the formation of **6** from the enol intermediate is speculative, but the formation of formic acid has been confirmed by HPLC. The proposed mechanism also accounts for the formation of the minor product **7**. Alternative mechanisms involve protein radicals (in contrast to just substrate radicals). Both mechanisms have been proposed for cofactor-independent oxygenases,[14] but the proposed mechanism or variations thereof that involve mainly general acid and base catalysis are more likely, particularly considering that DHNA is evolved for general acid and base catalysis.

The formation of **6** is enzyme-catalyzed and is not due to the spontaneous oxidation of the dissociated reaction intermediate **2**. The dissociation rate constants of substrate and product

(14) Fetzner, S. *Appl. Microbiol. Biotechnol.* **2002**, *60*, 243−257.

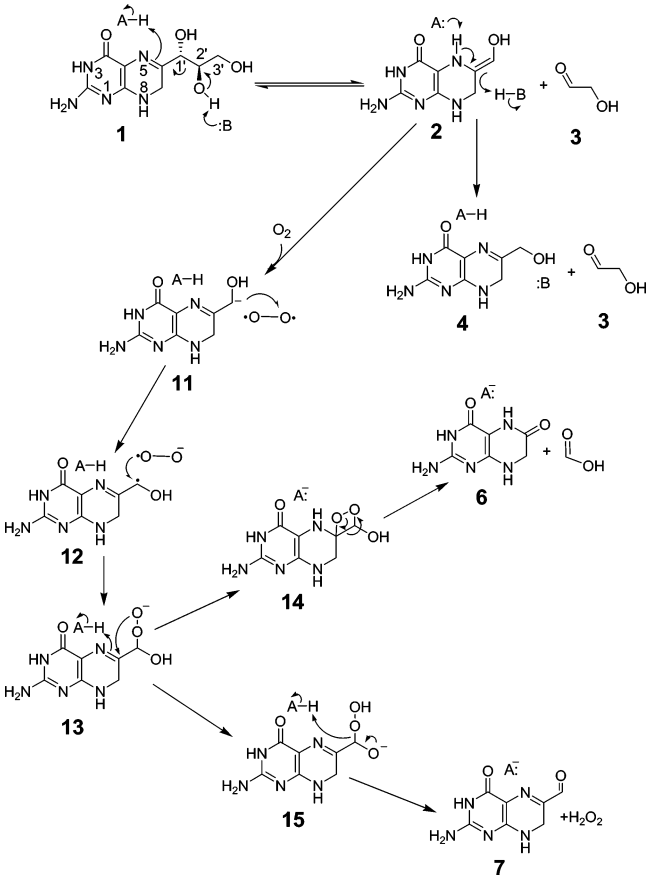

Figure 7. Proposed chemical mechanism for the generation of **6** and **7** by SaY54F and EcY53F. For simplicity, many steps are indicated by single arrows, irrespective of their reversibility.

analogues for SaY54F are lower than those for SaDHNA. Therefore, the dissociation rate constant for the reaction intermediate is most likely higher for the wild-type enzyme than for the mutant enzyme, although its value is not known for either the wild-type or the mutant enzyme. On the other hand, the rate for the formation of **6** is ~3% of that for the formation of **4** in the wild-type enzyme-catalyzed reaction. The relative rates are reversed in the mutant enzyme-catalyzed reaction, where the rate for the formation of **4** is ~2% of that for the formation of 7,8-dihydroxanthopterin (DHXP). The dissociated intermediate **2** most likely tautomerizes to form **4** rather than reacting with oxygen to form **6**.

The key step in the formation of **6** from the enol intermediate **2** is the generation of the carbanion species, which involves the deprotonation of N5 as in the wild-type enzyme-catalyzed reaction and the block of the protonation of the hydroxymethylene group by the mutation of the active-site tyrosine residue. Carbanions are prone to react with oxygen, and several enzymatic reactions involving carbanion intermediates indeed have oxygen-consuming side reactions.[15,16] The formation of the peroxide ion is reminiscent of the initial steps of the reactions catalyzed by 1*H*-3-hydroxy-4-oxoquinaldine 2,4-dioxygenase[17] and urate oxidase,[18,19] neither of which has any cofactor. These enzymes seem to evolve to utilize carbanion reactivity toward dioxygen for the oxygenation reactions,[14] which might be a general catalytic strategy for the family of cofactor-independent oxygenases. SaY54F and EcY54F are excellent examples for the evolution of such a cofactor-independent oxygenase. Interestingly, both DHNA[4,7,20,21] and urate oxidase[22,23] have a tunnel-like structure called a "T-fold" with active sites located between subunits.[24] The bound ligands are stacked with a conserved phenylalanine residue in urate oxidase and the conserved tyrosine in DHNA that was substituted with a phenylalanine residue in this study. Thus, individual folds are used by nature to catalyze many different kinds of reactions, as there might be no more than 1000 unique protein folds. Hence, it is possible to convert one enzyme to another by protein engineering. A recent example is the protein engineering of cycloartenol synthase, in which two site-directed mutations (H477N and I481V) convert the enzyme to lanosterol synthase.[25] In the present work, a single tyrosine-to-phenylalanine mutation converts DHNA to an oxygenase. In both cases, the protein folds are most likely preserved.

The Role of the Conserved Tyrosine Residue. The biochemical analysis of the two mutants SaY54F and EcY53F indicates that the hydroxyl group of the phenol ring of the conserved tyrosine residue plays only a minor role in the physical steps of the enzymatic reaction. In contrast, the hydroxyl group plays a critical role in catalysis. The hallmark of the DHNA-catalyzed reaction is general acid and base catalysis. The general acid and base involved in the protonation and deprotonation of N5 are most likely a water molecule and its conjugated base, based on the published crystal structures[7] and our own unpublished crystal structures. The deprotonation of the 2′-hydroxyl group is most likely the function of the conserved lysine residue, K100 in SaDHNA and K98 in EcDHNA. The conserved tyrosine residue may play a minor role if any in this step, because the formation of the enol intermediate is not impaired by the mutations to any great extent, as evidenced by the high k_{cat} for the formation of **6** by the mutant SaY54F, which is 1/10 of the k_{cat} value for the formation of **4** by the wild-type enzyme. On the other hand, the major product of the mutant-catalyzed reaction is **6**, not **4**, suggesting that the protonation of the enol intermediate to generate **4** is greatly impaired and the conserved tyrosine residue may play a critical role in this step. The high oxygenase activities of the mutants are likely due to the tendency of the enol intermediate to react with molecular oxygen and the available general acid and base for the generation of the enol intermediate and its subsequent oxygenation, as illustrated in Figure 7. The conserved tyrosine residue is located at the bottom of the active site. The active site is likely to be accessible to molecular oxygen, even in the wild-type enzyme. The wild-type enzyme is an efficient aldolase

(15) Abell, L. M.; Schloss, J. V. *Biochemistry* **1991**, *30*, 7883−7887.
(16) Hixon, M.; Sinerius, G.; Schneider, A.; Walter, C.; Fessner, W. D.; Schloss, J. V. *FEBS Lett.* **1996**, *392*, 281−284.
(17) Frerichs-Deeken, U.; Ranguelova, K.; Kappl, R.; Huttermann, J.; Fetzner, S. *Biochemistry* **2004**, *43*, 14485−14499.
(18) Sarma, A. D.; Tipton, P. A. *J. Am. Chem. Soc.* **2000**, *122*, 11252−11253.
(19) Imhoff, R. D.; Power, N. P.; Borrok, M. J.; Tipton, P. A. *Biochemistry* **2003**, *42*, 4094−4100.
(20) Bauer, S.; Schott, A. K.; Illarionova, V.; Bacher, A.; Huber, R.; Fischer, M. *J. Mol. Biol.* **2004**, *339*, 967−979.
(21) Goulding, C. W.; Apostol, M. I.; Sawaya, M. R.; Phillips, M.; Parseghian, A.; Eisenberg, D. *J. Mol. Biol.* **2005**, *349*, 61−72.
(22) Colloc'h, N.; ElHajji, M.; Bachet, B.; Lhermite, G.; Schiltz, M.; Prange, T.; Castro, B.; Mornon, J. P. *Nat. Struct. Biol.* **1997**, *4*, 947−952.
(23) Retailleau, P.; Colloc'h, N.; Vivares, D.; Bonnete, F.; Castro, B.; El Hajji, M.; Mornon, J. P.; Monard, G.; Prange, T. *Acta Crystallogr. Sect. D: Biol. Crystallogr.* **2004**, *60*, 453−462.
(24) Colloc'h, N.; Poupon, A.; Mornon, J. P. *Proteins* **2000**, *39*, 142−154.
(25) Lodeiro, S.; Schulz-Gasch, T.; Matsuda, S. P. T. *J. Am. Chem. Soc.* **2005**, *127*, 14132−14133.

rather than an oxygenase, because it has a general acid that can efficiently protonate the enol intermediate to form **4**.

Acknowledgment. This work was supported in part by NIH grant GM51901 (H.Y.) and Michigan State University Intramural Research Grant 04-IRGP-117 (G.E.R.). This study made use of a Varian INOVA-600 NMR spectrometer at Michigan State University, funded in part by NSF Grant BIR9512253. We are grateful to Dr. Yue Li for assistance in the site-directed mutagenesis experiments, Dr. Denise Mills for assistance in the oxygen consumption assay, Mr. James B. McKinlay for assistance in the HPLC identification of formic acid, the MSU Mass Spectrometry Facility for GC/MS analysis, and Drs. Robert P. Hausinger, J. Gregory Zeikus, and Kathleen A. Gallo for discussions and suggestions.

Supporting Information Available: Figures S1−S8, showing the binding of binding of **10** to EcY53F at equilibrium, the stopped-flow analysis of the binding of **9** to EcY53F, the ESI-MS/MS identification of **1**, **4**, **6**, **7**, and **10**, the GC/MS identification of **3**, and the HPLC identification of formic acid; complete ref 4. This material is available free of charge via the Internet at http://pubs.acs.org.

JA063455I